DOI: 10.1021/ma901676j

Macromolecules
ARTICLE

Extraordinary Wavelength Dispersion of Orientation Birefringence for Cellulose Esters

Masayuki Yamaguchi,* Kyoko Okada,† Mohd Edeerozey Abd Manaf, Yasuhiko Shiroyama, Takuya Iwasaki,‡ and Kenzo Okamoto

School of Materials Science, Japan Advanced Institute of Science and Technology, 1-1 Asahidai, Nomi, Ishikawa 923-1292 JAPAN. †Present address: Soken Chemical & Engineering Co., Ltd. ‡Present address: Suzuki Motor Corporation

Received July 29, 2009; Revised Manuscript Received September 30, 2009

ABSTRACT: Orientation birefringence and its wavelength dispersion are studied for hot-drawn films of cellulose esters such as cellulose triacetate (CTA), cellulose diacetate (CDA), cellulose acetate propionate (CAP), and cellulose acetate butyrate (CAB). The orientation birefringence of the cellulose esters is not proportional to the orientation function, indicating that the stress-optical law is not applicable for the cellulose esters. Furthermore, CTA shows negative birefringence, and the magnitude of the absolute value decreases with increasing the wavelength. On the contrary, CAP, CAB, and CDA show positive orientation birefringence that increases with the wavelength. The extraordinary wavelength dispersion of the orientation birefringence for CAP, CAB, and CDA is attributed to the difference in polarizability anisotropy of ester groups. Furthermore, the wavelength dependence of the orientation birefringence for CAP is dependent on the draw ratio and draw temperature, demonstrating that the contribution of polarizability anisotropy from each ester group to the orientation birefringence varies with the draw ratio and temperature. Moreover, the molecular weight and film-processing method also affect the orientation birefringence.

Introduction

Intensive efforts have been paid for the research and development of optical films these days because of the rapid growth of the market as well as the technology in the field of optical devices. In particular, a film having appropriate optical retardation, that is, the product of the birefringence and thickness, is desired for various applications such as liquid crystal display, electroluminescence display, and optical pick-up lens. Recent great progress in this field is a compensated film employing discotic liquid crystal and aromatic polyimide, which successfully leads to a wide-view angle for a twisted or supertwisted mode display.[1,2] Furthermore, the technical trend for the retardant film is to reduce the thickness and to adjust the retardation in the wide range of visible light. For example, a quarter-wave plate, one of the most important applications of retardant films, is required to exhibit the retardation of a quarter of the wavelength in a broad range of visible light. Therefore, the orientation birefringence has to increase with wavelength, which is unusual for conventional polymers.

On the basis of the Kuhn and Grün model proposed for the stress-optical behavior of cross-linked rubbers,[3,4] the orientation birefringence, $\Delta n(\lambda)$, of an oriented polymer is expressed as follows[3−7]

$$\Delta n(\lambda) = \frac{2\pi}{9}\frac{(n(\lambda)^2+2)^2}{n(\lambda)} N\Delta\alpha(\lambda)\left(\frac{3\langle\cos^2\theta\rangle - 1}{2}\right) \qquad (1)$$

where λ, $n(\lambda)$, N, $\Delta\alpha(\lambda)$, and θ are the wavelength of light, the average refractive index, the number of chains in a unit volume, the polarizability anisotropy, and the angle that a segment makes with the stretch axis, respectively. The last bracketed term $(3\langle\cos^2\theta\rangle - 1)/2$ is identically equal to the Hermans orientation function,[8] whereas the other part in the right term is called intrinsic birefringence, which is determined by chemical structure. Consequently, eq 1 can be written by

$$\Delta n(\lambda) = \Delta n^0(\lambda) F \qquad (2)$$

where $\Delta n^0(\lambda)$ is the intrinsic birefringence and F is the orientation function.

Because the orientation function is independent of the wavelength, the following simple relation is derived

$$\frac{\Delta n(\lambda)}{\Delta n(\lambda_0)} = \frac{\Delta n^0(\lambda)}{\Delta n^0(\lambda_0)} = \text{const} \qquad (3)$$

where λ_0 is the arbitrary standard wavelength.

According to eq 3, the wavelength dispersion of birefringence, that is, $\Delta n(\lambda)/\Delta n(\lambda_0)$, is a constant and is determined by the chemical structure of a polymer. Furthermore, it is known that $\Delta n(\lambda)/\Delta n(\lambda_0)$ of polymeric materials decreases with increasing wavelength in general, which is so-called ordinary dispersion. This is attributed to a strong absorption in ultraviolet region for polymers. The wavelength dispersion of the birefringence is, therefore, contrary to that of an ideal quarter-wave plate.

The extraordinary dispersion of the orientation birefringence is attained by piling two or more polymer films having different wavelength dispersions, in which the fast direction of one film is set to be perpendicular to the fast direction of the other film. Although this technique is currently employed, it leads to poor cost-performance because of the complicated processing operation and results in a thick display. Meanwhile, Uchiyama et al. investigated the optical anisotropy of oriented miscible polymer

*Corresponding author. Tel: +81-761-51-1621. Fax: +81-761-51-1625. E-mail: m_yama@jaist.ac.jp.

 Published on Web 10/29/2009

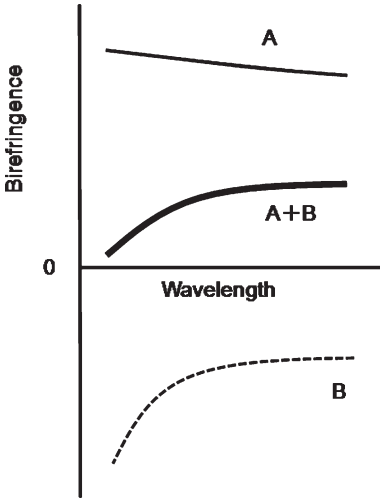

Figure 1. Schematic illustration of extraordinary dispersion of orientation birefringence for miscible polymer blend comprising of polymer (A) with positive birefringence and polymer (B) with negative birefringence.

blends composed of polystyrene (PS) and poly(2,6-dimethyl 1,4-phenylene oxide) (PPO) and found that the blend shows extraordinary dispersion.[9,10] In their technique, miscible polymer pairs having opposite sign of intrinsic birefringence are mixed and stretched. Because the orientation birefringence of multicomponent materials is determined by the addition of the contribution from each component,[5] the obtained film shows extraordinary wavelength dispersion, as illustrated in Figure 1. Recently, Kuboyama et al. carried out a similar work using miscible blends composed of polynorbornene (NB) and poly(styrene-*co*-maleic anhydride) (SMA) and demonstrated that the blend also exhibits the extraordinary dispersion of oriented birefringence.[11] They showed that the wavelength dependence of the birefringence is controlled by draw ratio, which was discussed in terms of the molecular orientation and relaxation of each component. This advanced research makes it possible to produce an extraordinary dispersion film without piling process.

The wavelength dispersion of the orientation birefringence for cellulose esters is discussed in this study considering the contribution of each ester group. It was clarified in our previous study that the orientation birefringence of cellulose esters is not determined by the orientation of pyranose ring but by the species and the amount of ester groups.[12] For example, the acetyl group provides negative orientation birefringence, whereas propionyl and butyryl groups contribute positive orientation birefringence with an intense fashion of the butyryl group. This situation is similar to the miscible blend systems showing extraordinary dispersion, such as PPO/PS and NB/SMA. Although some of the cellulose esters are currently employed for retardant films because of various attractive properties,[13−18] only a few papers on wavelength dispersion of the orientation birefringence have been published to the best of our knowledge.[12,19] However, it is inevitable to understand the wavelength dispersion, especially the effect of chemical structure, molecular weight, and processing method and condition, for material design of a retardant film.

Experimental Section

Materials. The materials employed in this study were commercially available cellulose esters such as cellulose acetate, cellulose acetate propionate (CAP), and cellulose acetate butyrate (CAB). Two types of cellulose acetate having different degrees of substitution of the acetyl group (DS_A) were purchased from Kanto Kagaku; CTA (DS_A = 2.96) and CDA (DS_A = 2.51). Furthermore, CAP and CAB employed were produced by Eastman Chemical. The molecular characteristics are summarized in Table 1. Although the covering range of the degree of substitution of ester groups and molecular weights is limited because of the commercially available samples, the experimental results will provide, at least, qualitative information on the effect of chemical structure and molecular weights.

Table 1. Characteristics of Samples[a]

sample	compositions, wt %			molecular weights	
	acetyl	propionyl/ butyryl	hydroxyl	$M_n \times 10^{-5}$	$M_w \times 10^{-5}$
CTA	43.6 (2.96)		0.9	1.3	3.5
CDA	38.0 (2.41)		3.7	n.d.[b]	n.d.[b]
CAP-482-20	2.5 (0.19)	46 (2.58)	1.8	0.77	2.1
CAB-171-15	29.5 (2.08)	17 (0.73)	1.1	0.62	2.7
CAB-381-20	13.5 (1.05)	37 (1.74)	1.8	0.68	3.0
CAB-381-0.5	13.5 (1.06)	38 (1.80)	1.3	0.21	1.2
CAB-551-0.2	2.0 (0.17)	52 (2.64)	1.8	0.082	0.78

[a](Parentheses): degree of substitution. [b] The sample is not dissolved in chloroform.

The molecular weights of the samples were evaluated using a gel permeation chromatograph (Tosoh, HLC-8020) with TSK-GEL GMHXL; chloroform was employed as the eluant, and its flow rate was 1.0 mL/min. The temperature was maintained at 40 °C, and the sample concentration was 1.0 mg/mL. The number- and weight-average molecular weights versus a PS standard are shown in the Table.

As seen in the Table, CAB-381-0.5 and CAB-381-20 have similar amounts of the acetyl and butyryl groups, although the molecular weight is significantly different. Therefore, the comparison of the two samples gives the information on the effect of molecular weight.

CAP and CAB were compressed into flat sheets by a compression-molding machine (Tester Sangyo, Table-type-test press SA-303-I-S) for 5 min at 200 °C under 10 MPa and subsequently plunged into an ice−water bath. In the case of CTA and CDA, however, the solution casting method was employed to prepare the film sample because melt processing is not applicable because of the severe thermal degradation.[13,18] The solvent employed was chloroform for CTA and tetrahydrofuran for CDA. The initial concentration was 6 wt %. We obtained the film with ~200 μm thickness by evaporating the solvent at room temperature. Furthermore, another film of CAP-482-20 was also prepared by the solution casting method employing chloroform as solvent to comprehend the effect of the processing method on the orientation birefringence.

The melting point and heat of fusion of the obtained films were measured by a differential scanning calorimeter (Mettler, DSC820) at a heating rate of 30 °C/min. The results are shown in Table 2.

The uniaxial oriented films were prepared by hot-drawing operation using a dynamic mechanical analyzer (UBM, DVE-4) at various temperatures and draw ratios. The initial distance between the clumps was 10 mm, and the stretching rate was 0.5 mm/s. The drawn sample was quenched by blowing cold air to avoid relaxation of molecular orientation.

Measurements. The temperature dependence of oscillatory tensile moduli in the solid state, such as storage modulus E', loss modulus E'', and loss tangent tan δ, was measured from −50 to 200 °C using a dynamic mechanical analyzer (UBM, E-4000). The frequency and heating rate used were 10 Hz and 2 °C/min, respectively. The rectangular specimen, in which the width is 3.0 mm and the length is 15 mm, was employed.

Table 2. Melting Points and Average Refractive Index of Film Samples

sample	melting point and heat of fusion	average refractive index
CTA	287 °C, 21.8 J/g	1.48 ± 0.01*
CDA	n.d.	1.475 ± 0.001*
CAP-482-20 (compression-molding)	199 °C, 0.7 J/g	1.4738
CAP-482-20 (solution cast)	152 °C, 1.6 J/g	1.4738
CAB-171-15	n.d.	1.4758
CAB-381-20	n.d.	1.4744
CAB-381-0.5	n.d.	1.4743
CAB-551-0.2	n.d.	1.4737

*Refractive indices of CTA and CDA have large experimental errors.

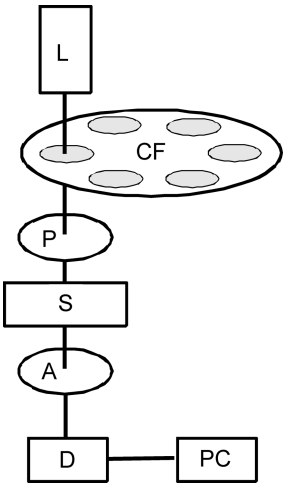

Figure 2. Schematic diagrams of the retardation measurement: L, halogen lamp; CF, color filters; P, polarizer; S, sample film; A, analyzer; D, detector; PC, computer.

The refractive index of the polymer films was evaluated by an Abbe refractometer (Atago, NRA 1T) at room temperature employing α-bromonaphthalene as a contact liquid.

The birefringence of the drawn films was measured at room temperature by an optical birefringence analyzer (Oji Scientific Instruments, Inc., KOBRA-WPR) as a function of wavelength by changing color filters. The diagram of the measurement is illustrated in Figure 2.

The infrared dichroism of the stretched specimens was evaluated by a Fourier transform infrared spectrometer (JASCO, FT-IR 6100) equipped with a polarizer. The absorbance of the band at 880 cm^{-1}, which is assigned to the pyranose ring,[12,20,21] was measured by a linearly polarized IR beam whose electric vector is parallel $A_{\parallel}$ and perpendicular $A_{\perp}$ to the stretching direction.

Results and Discussion

Orientation Birefringence of CAP. We measured the temperature dependence of the oscillatory tensile moduli, such as storage modulus E', loss modulus E'', and loss tangent tan δ, to decide the ambient temperature at hot-drawing. Figure 3 exemplifies the dynamic mechanical spectra for the compressed film of CAP-482-20 at 10 Hz, which is a typical one for a glassy polymer. As seen in the Figure, the glass-transition temperature, T_g, which is defined as the peak temperature in the E'' curve, is ~148 °C. Furthermore, the storage modulus E' falls off sharply around T_g.

Figure 4 shows the wavelength dispersion of the orientation birefringence for the compressed film of CAP-482-20 at various draw ratios. The hot-drawing was performed at the

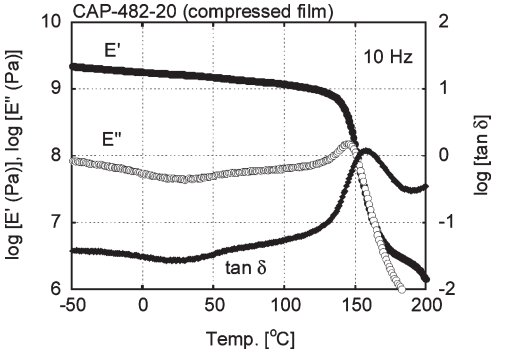

Figure 3. Temperature dependence of oscillatory tensile moduli such as storage modulus E' (○), loss modulus E'' (●), and loss tangent tan δ (◆) for a CAP-482-20 film obtained by compression molding at 10 Hz.

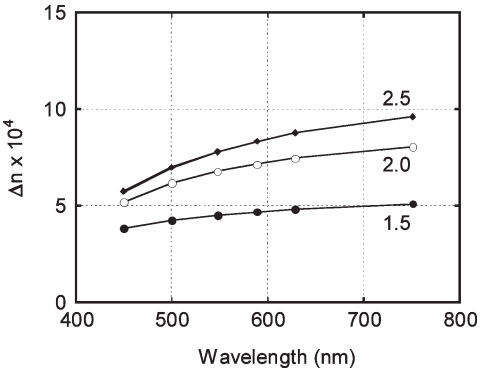

Figure 4. Wavelength dependence of orientation birefringence $\Delta n(\lambda)$ for stretched films of CAP-482-20 at various draw ratios; 1.5 (●), 2.0 (○), and 2.5 (◆). Hot-drawing was performed at 163 °C. The films were prepared by compression molding.

temperature where the tensile storage modulus at 10 Hz was 10 MPa (163 °C). As increasing the draw ratio, the orientation birefringence increases. Furthermore, it should be noted that the orientation birefringence of CAP-482-20 increases with the wavelength, that is, extraordinary dispersion.

Infrared birefringence is also measured for the samples to evaluate the contribution of the orientation of the pyranose ring, that is, the main chain of cellulose esters. It is well known that the orientation function is expressed by the dichroic ratio D ($\equiv A_{\perp}/A_{\parallel}$) as follows

$$F = c\frac{D-1}{D+2} \tag{4}$$

where c is a correction for the inclination of the transition moment direction of the band from the molecular axis. Because c can be assumed to be a constant irrespective of the orientation of the ester groups, Δn is proportional to $(D-1)/(D+2)$ as long as the stress-optical law is applicable.

As demonstrated in Figure 5, however, the stress-optical law is not applicable to CAP-482-20, indicating that the orientation of the main chains is not responsible for the orientation birefringence for cellulose esters. This result corresponds to our preceding study, in which the orientation birefringence of cellulose esters is found to be determined mainly by the contribution of ester groups.[12] Moreover, the acetyl group provides negative orientation birefringence, whereas the propionyl and butyryl groups give positive orientation birefringence with an intense fashion of the butyryl group.[12] The flexible and bulky methylene part in ester groups would lead to the parallel orientation of the

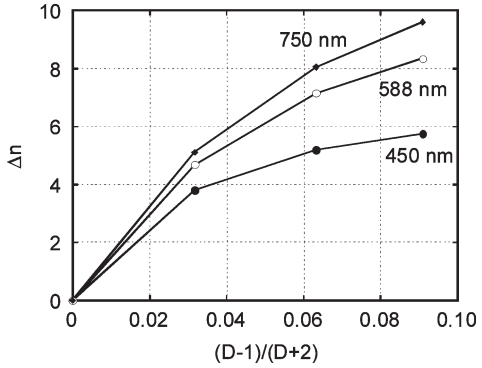

Figure 5. Relationship between (D − 1)/(D + 2) and orientation birefringences at 450 (●), 588 (○), and 750 nm (◆) or stretched films of CAP-482-20. The films were prepared by compression molding.

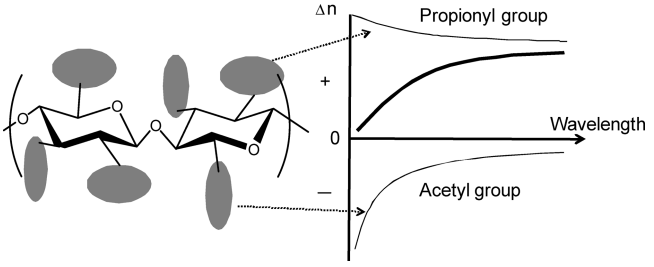

Figure 6. Schematic illustration of contribution of polarizability anisotropy of acetyl and propionyl groups and the obtained wavelength dispersion of oriented birefringence for CAP.

polarizability anisotropy along the flow direction. Furthermore, the interaction between the ester groups and the main chains may be important because the higher-order structure of cellulose esters[13,14,18] is strongly dependent on the species of the ester groups. To comprehend the detail, further study employing model polymers whose distribution of ester groups is well characterized will be required. Moreover, the detailed characterization on the orientation of the specific segments, such as the esters and hydroxyl group, is needed for the quantitative discussion.

As is well known, CAP has at least two ester groups having different polarizability anisotropies, that is, acetyl and propionyl groups. Because the orientation birefringence, Δn, is assumed to be expressed by a simple addition of the birefringence from each component, as discussed by Stein et al.,[5,22] it is provided by the following relation

$$\Delta n = \Delta n_{\mathrm{F}} + \sum_i \phi_i \Delta n_i \tag{5}$$

where i refers to the ith component, ϕ_i is the volume fraction, and Δn_{F} is the birefringence arising from form or deformation effects, which is negligible for cellulose esters owing to the homogeneous structure. Therefore, the orientation birefringence is determined by the summation of the birefringences arising from the acetyl group and that from the propionyl group as expressed in the following relation

$$\Delta n(\lambda) = \Delta n_{\mathrm{A}}{}^{0}(\lambda) F_{\mathrm{A}} + \Delta n_{\mathrm{P}}{}^{0}(\lambda) F_{\mathrm{P}} \tag{6}$$

where $\Delta n_{\mathrm{A}}^{0}(\lambda)$ and $\Delta n_{\mathrm{P}}^{0}(\lambda)$ are the intrinsic birefringences and F_{A} and F_{P} are the orientation functions of the acetyl and propionyl groups, respectively. The extraordinary wavelength dispersion of the orientation birefringence with positive sign for CAP-482-20 is explained by the illustration in Figure 6. The polarizability anisotropy of ester groups is represented by ellipsoids here. As qualitatively shown in the plot of the birefringence, the addition of both components, denoted by a bold line, gives the extraordinary dispersion with positive orientation birefringence when the wavelength dependence of the propionyl group is weaker than that of the acetyl group. This would be a similar situation to Figure 1, although the current experiments reveal that only one polymeric material, not polymer blends, exhibits extraordinary dispersion.

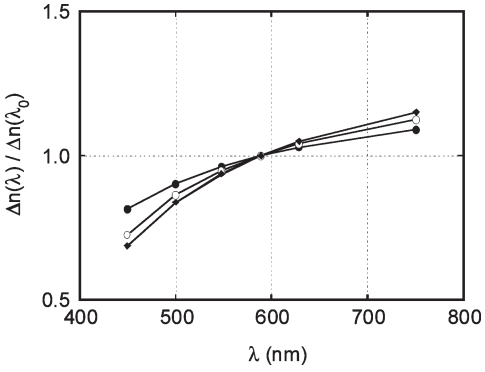

Figure 7. Normalized wavelength dependence of orientation birefringence $\Delta n(\lambda)/\Delta n(\lambda_0 = 588\ \mathrm{nm})$ for stretched films of CAP-482-20 at various draw ratios; 1.5 (●), 2.0 (○), and 2.5 (◆). The films were prepared by compression molding.

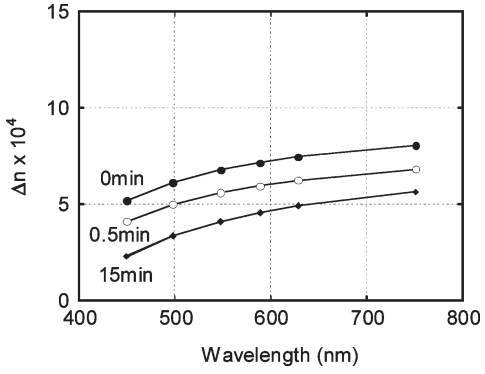

Figure 8. Wavelength dependence of orientation birefringence $\Delta n(\lambda)$ for stretched films of CAP-482-20 with various holding times after hot-drawing; immediately cooled after hot-drawing (●), cooled after holding for 0.5 min (○), and cooled after holding for 15 min (◆). Hot-drawing (draw ratio was 2.0) and subsequent holding procedures were performed at 163 °C. The films were prepared by compression molding.

Moreover, Figure 5 suggests that the orientation birefringence at light with short wavelength deviates significantly from the linear relationship, suggesting that the wavelength dispersion depends on the draw ratio. Figure 7 shows the normalized orientation birefringence, that is, $\Delta n(\lambda)/\Delta n(\lambda_0 = 588\ \mathrm{nm})$, for the compressed films of CAP-482-20 with various draw ratios. As demonstrated, the extraordinary dispersion is pronounced as increasing the draw ratio. Considering that the acetyl group shows the strong wavelength dispersion, as illustrated in Figure 6, the experimental result indicates that the contribution of the acetyl group, that is, $F_{\mathrm{A}}/(F_{\mathrm{A}} + F_{\mathrm{P}})$, increases with the draw ratio. On the contrary, the propionyl group greatly contributes to the orientation birefringence at low draw ratio, suggesting that the orientation of the propionyl group occurs even at low stress.

Figure 8 shows the effect of the postdrawing stress/orientation relaxation on the wavelength dispersion of the orientation birefringence for the compressed film of CAP-482-20. In this experiment, the drawn sample was kept at the ambient

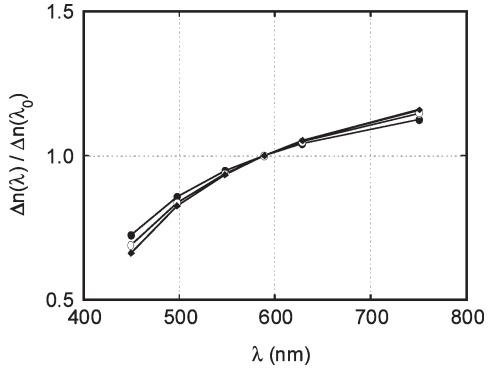

Figure 9. Normalized wavelength dependence of orientation birefringence $\Delta n(\lambda)/\Delta n(\lambda_0 = 588$ nm) for stretched films of CAP-482-20 with various holding times after hot-drawing; immediately cooled after hot-drawing (●), cooled after holding for 0.5 min (○), and cooled after holding for 15 min (◆). Hot-drawing (draw ratio was 2.0) and subsequent holding procedures were performed at 163 °C. The films were prepared by compression molding.

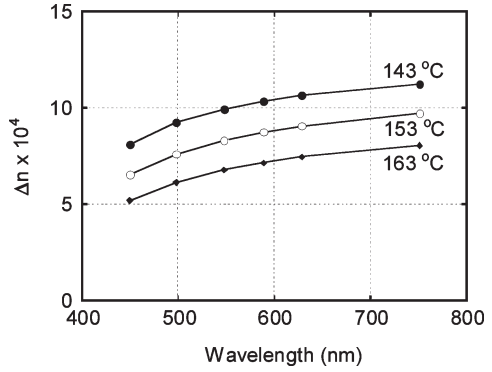

Figure 10. Wavelength dependence of orientation birefringence $\Delta n(\lambda)$ for stretched films of CAP-482-20 at various temperatures; 143 (●), 153 (○), and 163 °C (◆) at a draw ratio of 2.0. The films were prepared by compression molding.

temperature 163 °C maintaining the strain for 0, 0.5, and 15 min prior to the cooling by blowing air. Apparently, the immediate cooling after the hot-drawing procedure (0 min), which was employed in other experiments, provides the highest orientation birefringence. Then, it decreases with increasing holding time owing to the relaxation of the orientation. Furthermore, the plot of the normalized orientation birefringence as a function of the wavelength, as seen in Figure 9, demonstrates that the extraordinary dispersion is enhanced after relaxation, suggesting that the orientation of the propionyl group relaxes faster than that of the acetyl group. Consequently, the contribution of the acetyl group to the orientation birefringence, that is, $F_A/(F_A + F_P)$, is pronounced after relaxation.

The effect of the hot-drawing temperature on the orientation birefringence and the degree of the extraordinary dispersion are shown in Figures 10 and 11, respectively. The orientation birefringence is found to increase with lowering the temperature. This is reasonable because the orientation of the ester groups will be strong at low temperature, in accordance with that of the main chain. Furthermore, the extraordinary dispersion is pronounced at the sample drawn at high temperature, as seen in Figure 11, which corresponds with the result in Figure 8. Because of the orientation relaxation of the ester groups during the hot-drawing, in which the propionyl group relaxes faster than the acetyl group, the extraordinary dispersion becomes strong for the sample drawn at high temperature.

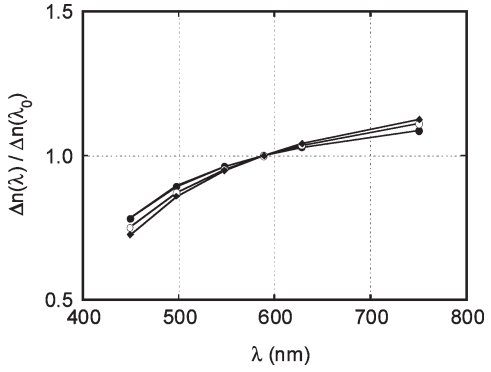

Figure 11. Normalized wavelength dependence of orientation birefringence $\Delta n(\lambda)/\Delta n(\lambda_0 = 588$ nm) for stretched films of CAP-482-20 at various temperatures; 143 (●), 153 (○), and 163 °C (◆) at a draw ratio of 2.0. The films were prepared by compression molding.

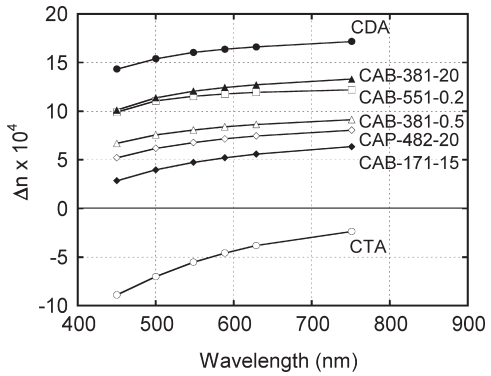

Figure 12. Wavelength dependence of orientation birefringence for various samples at a draw ratio of 2.0; CTA (○), CDA (●), CAP-482-20 (compressed film) (◇), CAB-171-15 (◆), CAB-381-0.5 (△), CAB-381-20 (▲), and CAB-551-0.2 (□). Hot-drawing was performed at the temperature where the tensile storage modulus is 10 MPa at 10 Hz.

Effect of Chemical Structure and Molecular Weight. Figure 12 shows the wavelength dispersion of the orientation birefringence for various cellulose esters at a draw ratio of 2. The hot-drawing was performed at the temperature where the tensile storage modulus at 10 Hz was 10 MPa for all samples except for CTA and CDA. In the case of CTA and CDA, the hot-drawing was performed at 205 °C. The film of CAP-482-20 was prepared by the compression molding.

It is apparent from Figure 12 that the orientation birefringence is dependent on the species and the contents of the ester groups as well as the molecular weight. The orientation birefringence seems to increase with the butyryl content in CAB, although CAB-381-20 shows higher orientation birefringence than CAB-551-0.2.

In general, as demonstrated in eq 1, the orientation birefringence is determined by the product of the orientation function and the intrinsic birefringence, which is provided by the average refractive index and the polarizability anisotropy. Table 2 shows the refractive index of the sample films. Obviously, the refractive index decreases with increasing the butyryl content in CAB. Furthermore, the refractive index of CAP-482-20 is lower than that of CAB-171-15. These experimental results cannot explain the order of the orientation birefringence in Figure 12. Therefore, it is deduced that the polarizing anisotropy would decide the orientation birefringence of cellulose esters as well as the orientation of each ester group.

Figure 12 clarifies that the absolute value of the orientation birefringence decreases with the wavelength for CTA

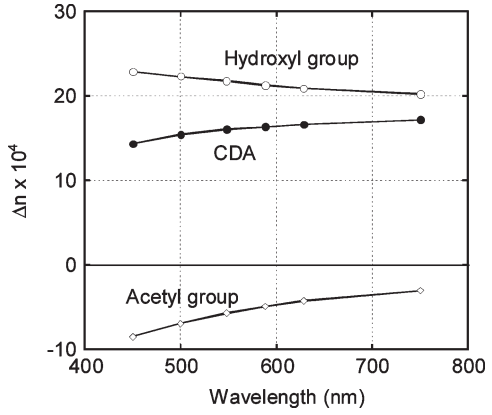

Figure 13. Contribution of hydroxyl (○) and acetyl (◇) groups to orientation birefringence of CDA (●) at a draw ratio of 2.0. The birefringences of both groups are calculated from the experimental results of CTA and CDA.

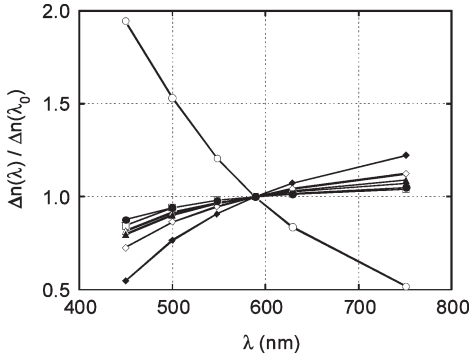

Figure 14. Normalized wavelength dependence of orientation birefringence $\Delta n(\lambda)/\Delta n(\lambda_0 = 588\ \text{nm})$ for various samples at a draw ratio of 2.0; CTA (○), CDA (●), CAP-482-20 (compressed film) (◇), CAB-171-15 (◆), CAB-381-0.5 (△), CAB-381-20 (▲), and CAB-551-0.2 (□). Hot-drawing was performed at the temperature where the tensile storage modulus is 10 MPa at 10 Hz.

(ordinary dispersion), as reported by El-Diasty et al.[19] This is a typical phenomenon for most conventional polymers. On the contrary, extraordinary wavelength dispersion of the orientation birefringence is detected for CDA, CAP, and CAB. Furthermore, CAB-381-20 shows higher orientation birefringence than CAB-381-0.5, although the chemical structure is almost similar. The difference will be attributed to the relaxation during the hot-drawing. Because CAB-381-0.5 has lower molecular weight, that is, shorter relaxation time, the orientation relaxes to a great extent. It is well known that the average relaxation time is proportional to $M^{3.4}$. Consequently, the relaxation time of CAB-381-20 is ~40 times as long as that of CAB-381-0.1. The same discussion is applicable for CAB-551-0.2. Although CAB-551-0.2 has a high content of the butyryl group, which enhances the positive orientation birefringence, the rapid relaxation occurs during the hot-drawing because of the low molecular weight, which leads to a low level of orientation birefringence. Figure 12 also demonstrates that CDA shows large positive values of the orientation birefringence. The result indicates that the hydroxyl group contributes positive birefringence to a great extent. Because the contribution of the hydroxyl group is significantly stronger than that of the butyryl group, it is impossible to discuss the contribution of the acetyl, propyonyl, and butyryl groups in CAP and CAB quantitatively without the information on the exact amount of the hydroxyl group.

Assuming (1)−(4), the contributions of hydroxyl and acetyl groups in CDA are calculated from the experimental results of CTA and CDA using the same relation of eq 6: (1) relaxation of the orientation is ignored, (2) contribution of the main chain to the birefringence is ignored, (3) contribution of the crystalline part of CTA to the birefringence is ignored, and (4) both hydroxyl and acetyl groups have the same orientation function in CTA and CDA at a constant draw ratio. As seen in Figure 13, great contribution of the hydroxyl group is confirmed, although the molar content in CDA is lower than that of the acetyl group. Furthermore, the acetyl group shows strong wavelength dispersion, which is discussed in Figure 14.

The normalized orientation birefringence is shown in Figure 14. It is demonstrated that both CAB-381-20 and CAB-381-0.5 show almost similar normalized orientation birefringence, whereas the absolute value of the orientation birefringence is considerably different. The slight difference in the wavelength dispersion between CAB-381-20 and CAB-381-0.5 would be attributed to the relaxation of ester groups, as discussed in Figure 9. Furthermore, the wavelength dependence of the normalized orientation function becomes weak as the butyryl content is increased. This is reasonable because the butyryl group has weak dependence on the wavelength.

Figure 14 also indicates that the slope of the orientation birefringence for CAP-482-20 is larger than that for CAB-551-0.2, although both contain a similar level of the degree of substitution of ester groups such as propionyl and butyryl groups. It suggests that the birefringence of the propionyl group shows strong dependence on the wavelength as compared with that of the butyryl group.

As a result, the following relation is expected.

$$-\left.\frac{\mathrm{d}(\Delta n(\lambda))}{\mathrm{d}\lambda}\right|_{\text{acetyl}} > \left.\frac{\mathrm{d}(\Delta n(\lambda))}{\mathrm{d}\lambda}\right|_{\text{propionyl}} > \left.\frac{\mathrm{d}(\Delta n(\lambda))}{\mathrm{d}\lambda}\right|_{\text{butyryl}} \quad (7)$$

It is generally accepted that wavelength dependence of the orientation birefringence of a polymeric material is well described by the following Sellmeier-type relation[6,23,24]

$$\Delta n(\lambda) = A + \frac{B}{\lambda^2 - \lambda_{\text{ab}}{}^2} \quad (8)$$

where λ_{ab} is the coefficient having the relation with the wavelength of a strong vibrational absorption peak in ultraviolet region and A and B are the Sellmeier coefficients.

In the case of cellulose esters, eq 7 is predictable because λ_{ab} of the ester groups is in the following order: acetyl > propionyl > butyryl.

Effect of Processing Method

As mentioned in the Introduction, large amounts of birefringence-controlled films are produced by solution casting method, not by extrusion. Therefore, the comprehension of the difference in the processing method would be important in the field. Table 2 shows that the degree of crystallization and the melting point of CAP-482-20 are dependent on the processing method. Although the pure powder shows a large amount of heat of fusion, 13.8 J/g at 200 °C, the solution cast sample has small heat of fusion (1.6 J/g) with low melting point (152 °C). The film obtained by the compression molding shows almost the same melting point,

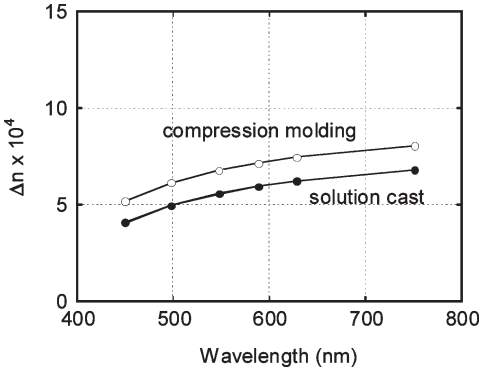

Figure 15. Wavelength dependence of orientation birefringence $\Delta n(\lambda)$ for CAP-482-20 films obtained by compression-molding (○) and solution cast (●). The draw ratio was 2.0.

199 °C, of the original powder, whereas the melting enthalpy is considerably small (0.7 J/g). Because the stretching is performed at 163 °C, the crystals play an important role in the orientation, even though the amount is considerably small. In the case of the film obtained by the solution cast, the crystals will disappear during the preheating. As a result, the molecular orientation is not as high as that of the compressed film, as shown in Figure 15. In other words, the degree of crystals and the melting point, which are decided by the processing method and condition, have to be seriously taken into consideration.

Conclusions

Orientation birefringence of various types of cellulose esters and its dependence of the wavelength are studied. The species and contents of ester groups determine the sign and magnitude of the orientation birefringence as well as the wavelength dispersion. It is found that CTA films show ordinary dispersion with negative birefringence. On the contrary, the orientation birefringence increases with increasing wavelength for CDA, CAP, and CAB, which is desired for a retardant film covering a broad wavelength. The difference in the sign of birefringence and the dependence of wavelength for the ester and hydroxyl groups are responsible for the extraordinary dispersion. Furthermore, CAP shows strong dependence of the orientation birefringence as compared with CAB, because the propionyl group gives stronger wavelength dependence than the butyryl group. Moreover, the wavelength dispersion is dependent on the draw ratio. It is attributed to the change of the contribution of polarizing anisotropy from each ester group. In particular, the contribution from the acetyl group becomes important at high draw ratio and after stress relaxation. The drawn films in which the acetyl group greatly contributes to the orientation birefringence exhibit the marked extraordinary wavelength dispersion. Molecular weight is another important factor to determine the orientation birefringence because it affects the relaxation behavior to a great extent. Finally, the degree of crystallization has to be carefully considered because it affects the degree of orientation. In the case of CAP-482-20, the processing method has an influence on the crystalline state of the film and thus the orientation birefringence.

Acknowledgment. We express our gratitude to Taihei Chemicals Limited for their valuable advice and the kind supply of the samples employed in this study. Furthermore, we gratefully acknowledge financial support from Regional Research and Development Resources Utilization Program, Japan Science and Technology Agency.

References and Notes

(1) Mori, H.; Itoh, Y.; Nishikawa, Y.; Nakamura, T.; Shinagawa, Y. *Jpn. J. Appl. Phys.* **1997**, *36*, 143–147.
(2) Mori, H.; Bos, P. J. *Jpn. J. Appl. Phys.* **1999**, *38*, 2837–2844.
(3) Kuhn, W.; Grun, F. *Kolloid Z.* **1942**, *101*, 248–271.
(4) Treloar, L. R. G. *The Physics of Rubber Elasticity*; Clarendon Press: Oxford, U.K., 1958.
(5) Read, B. E. Chapter 4. In *Structure and Properties of Oriented Polymers*; Ward, I. M., Ed.; Elsevier Applied Science Publishers: London, 1975.
(6) Harding G. F. Chapter 2. In *Optical Properties of Polymers*; Meeten, G. H., Ed.; Elsevier Applied Science Publishers: London, 1986.
(7) Marks, J. E.; Erman, B. *Rubberlike Elasticity: A Molecular Primer*; Wiley: New York, 1988.
(8) Hermans, P. H.; Platzek, P. *Kolloid Z.* **1939**, *88*, 68–72.
(9) Uchiyama, A.; Yatabe, T. *Jpn. J. Appl. Phys.* **2003**, *42*, 3503–3507.
(10) Uchiyama, A.; Yatabe, T. *Jpn. J. Appl. Phys.* **2003**, *42*, 5665–5669.
(11) Kuboyama, K.; Kuroda, T.; Ougizawa, T. *Macromol. Symp.* **2007**, *249*, 641–646.
(12) Yamaguchi, M.; Iwasaki, T.; Okada, K.; Okamoto, K. *Acta Mater.* **2009**, *57*, 823–829.
(13) Charles, K. J.; Buchanan, C. M.; Debenham, J. S.; Rundquist, P. A.; Seiler, B. D.; Shelton, M. C.; Tindall, D. *Prog. Polym. Sci.* **2001**, *26*, 1605–1688.
(14) Sata, H.; Murayama, M.; Shimamoto, S. *Macromol. Symp.* **2004**, *208*, 323–334.
(15) Kamide, K. *Cellulose and Cellulose Derivatives*; Elsevier Science: Amsterdam, 2005.
(16) Yamaguchi, M.; Masuzawa, K. *Eur. Polym. J.* **2007**, *43*, 3277–3282.
(17) Yamaguchi, M.; Masuzawa, K. *Cellulose* **2008**, *15*, 17–22.
(18) Zugenmaier, P. *Macromol. Symp.* **2004**, *208*, 81–166.
(19) El-Diasty, F.; Soliman, M. A.; Elgendy, A. F. T.; Ashour, A. *J. Opt. A: Pure Appl. Opt.* **2007**, *9*, 247–252.
(20) Kaputskii, V. E.; Komar, V. P.; Skornyakov, I. V. *J. Appl. Spectrosc.* **1988**, *48*, 257–260.
(21) Guo, Y.; Wu, P. *Carbohydr. Polym.* **2008**, *74*, 509–513.
(22) Stein, R. S.; Onogi, S.; Sasaguri, K.; Keedy, D. A. *J. Appl. Phys.* **1963**, *34*, 80–89.
(23) Ghosh, G. *Opt. Commun.* **1999**, *163*, 95–102.
(24) Scharf, T. *Polarized Light in Liquid Crystals and Polymers*; Wiley: New York, 2006.